4838 J. Med. Chem. 2009, 52, 4838–4843
DOI: 10.1021/jm900610k

Journal of Medicinal Chemistry Article

Structural Basis of Serine/Threonine Phosphatase Inhibition by the Archetypal Small Molecules Cantharidin and Norcantharidin†

I. Bertini,*[,§,‡] V. Calderone,[‡] M. Fragai,[‡,∥] C. Luchinat,[‡,∥] and E. Talluri[‡]

[‡]*Magnetic Resonance Center (CERM), University of Florence, Via L. Sacconi 6, 50019 Sesto Fiorentino, Italy,* [§]*Department of Chemistry, University of Florence, Via della Lastruccia 3, 50019 Sesto Fiorentino, Italy, and* [∥]*Department of Agricultural Biotechnology, University of Florence, Via Maragliano 75-77, 50144 Florence, Italy*

Received May 8, 2009

The inhibition of a subgroup of human serine/threonine protein phosphatases is responsible for the cytotoxicity of cantharidin and norcantharidin against tumor cells. It is shown that the anhydride rings of cantharidin and norcantharidin are hydrolyzed when bound to the catalytic domain of the human serine/threonine protein phosphatases 5 (PP5c), and the high-resolution crystal structures of PP5c complexed with the corresponding dicarboxylic acid derivatives of the two molecules are reported. Norcantharidin shows a unique binding conformation with the catalytically active Mn_2PP5c, while cantharidin is characterized by a double conformation in its binding mode to the protein. Different binding modes of norcantharidin are observed depending of whether the starting ligand is in the anhydride or in the dicarboxylic acid form. All these structures will provide the basis for the rational design of new cantharidin-based drugs.

Introduction

Cantharidin, the active constituent of the dried body blister beetles,[1] is a toxin displaying severe effects on the gastrointestinal tract, kidney, and ureter.[2] Nevertheless, it has been used in medicine for over 2000 years against cancerous skin lesions, as an aphrodisiac, abortifacient, and to treat ulcers and cervical tuberculous lymphadenopathy.[3,4] Cantharidin and its demethylated form, norcantharidin, are also effective against multidrug-resistant leukemia,[5] hepatoma,[6] and myeloma cells.[7] Norcantharidin is less toxic than cantharidin and is in clinical use in China since the 1980s to treat human cancers.[8] Cantharidin and norcantharidin are cyclic anhydrides.[1,9] Their structures are reported in Figure 1, together with the structures of their open dicarboxylic acid forms, cantharidic acid and endothall, respectively.

Cantharidin and its derivatives act by causing cell death. Many of the proposed mechanisms involve response to DNA damage and apoptosis through the inhibition of protein phosphatases.[10,11] Indeed, like sulfonamides for carbonic anhydrase[12] or hydroxamic acids for metalloproteinases,[13] cantharidin and norcantharidin are the archetypal small molecule protein phosphatase inhibitors.[1,14,15] Phosphatases are, together with kinases,[16] among the most studied targets in today's drug discovery programs.[17−19] It is therefore surprising that the structure of a complex between any of the four molecules shown in Figure 1 and any phosphatase has never been reported.

Protein phosphatases (PPs[a]) are metalloproteins with a dimetallic active site in the catalytic domain.[20] They can be divided in protein serine/threonine phosphatases and in protein tyrosine phosphatases, according to their substrate specificity. Protein serine/threonine phosphatases can be further classified into three groups on the basis of sequence, structure, and catalytic mechanism. The largest, named phospho protein phosphatases (PPP), comprises PP1, PP2A, PP2B, PP4, PP5, PP6, and PP7.[20−23] Cantharidin is a strong inhibitor of this group of phosphatases. The consensus sequence $(DXH(X)_nGDXXD(X)_mGNHD/E)$, highly conserved in the catalytic domain of these phosphatases,[24] contains most residues that coordinate the two metal ions in the active site and is considered as the signature of the PPP family.[25] The catalytic domain of PP5 (PP5c) shares 35−45% sequence identity with the catalytic domains of the other members of the group.[26] Therefore, PP5 can be considered not only a therapeutic target[27] but also a suitable general model to investigate the structural basis of the inhibition of PPP by cantharidin and its derivatives. Indeed, superposition of the available structures of PP5c containing endogenous (regulatory peptide)[28] or exogenous (phosphate)[29] ligands onto the structures of the catalytic domains of other eukaryotic phosphatases such as PP1,[30,31] PP2A,[32] and PP2B[33] gives root-mean-square deviations (rmsd) of < 2.0 Å within the highly homologous ∼270-residue region used in the calculations and even smaller rmsd (0.48 Å) if the superposition is limited to the active site.

†Coordinates and structure factors have been deposited at the Protein Data Bank. PDB ID codes: 3H60, 3H61, 3H62, 3H63, 3H64, 3H66.

*To whom correspondence should be addressed. Phone: +39 055 4574270. Fax: +390554574271. E-mail: bertini@cerm.unifi.it. Web site: www.cerm.unifi.it.

[a]Abbreviations: PPs, protein phosphatases; PPP, phospho protein phosphatases; PP5, serine/threonine protein phosphatases 5; ICP-MS, inductively coupled plasma mass spectrometry; pNPP, *p*-nitro-phenyl-phosphate.

 Published on Web 07/14/2009

Cantharidin is not the only natural toxin showing strong inhibition of phosphatases. Okadaic acid, microcystins, calyculin A, tautomycin, and fostriecin are among the most investigated toxins.[34] For several of them, the structures of the complexes with one or another serine-threonine phosphatase have been solved.[30,31,35−38] In all cases, these molecules occupy a relatively long groove on the surface of the catalytic site but do not form coordination bonds with the catalytic metals despite the presence of potentially metal-coordinating dicarboxylic acids in some of them. Furthermore, the molecular weights of these toxins are in the range 500−1000 Da, i.e., much higher than cantharidin and norcantharidin (196 and 168 Da, respectively). Therefore these complexes with large toxin molecules are of little help in predicting the structure of the cantharidin−phosphatase complex. At variance with these relatively large molecular weight toxins, cantharidin may be able to bind at the metal site, and several model structures have been proposed.[30,39−41] Experimental evidence for the displacement of the metal bound water molecule by cantharidin binding has been recently obtained,[42] supporting direct metal coordination.

We report here the X-ray structures of PP5c in the presence of all four ligands in Figure 1. The obtained structures show (i) that the anhydrides are hydrolyzed to cantharidic acids upon binding, (ii) two slightly different conformations of the bound molecules can be obtained for cantharidic acid, differing by the orientation of the metal-bound carboxylic groups, while (iii) two strikingly different conformations are found for endothall depending on whether PP5c is reacted with the anhydride or with the dicarboxylic acid form. All these structures provide the basis for the rational design of more specific, and thus possibly less toxic, cantharidin-like drugs. The structure of PP5c with an exposed bimetallic active site has been also solved for the first time in this work and is reported for comparison.

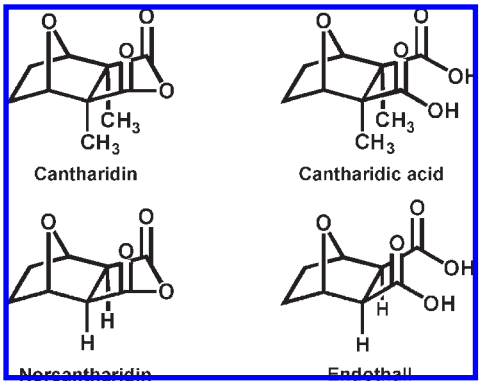

Figure 1. Structures of cantharidin, norcantharidin together with their open dicarboxylic acid forms, cantharidic acid and endothall, respectively.

Results and Discussion

Free Enzyme Structures. The catalytic domain of PP5 was expressed as previously reported.[42] The protein was dialyzed against either Mn^{2+} or Zn^{2+} solutions until Mn_2PP5c or Zn_2PP5c were formed, as judged by ICP-MS and atomic absorption. As for several other phosphatases the Mn_2 form is active against the test substrate *p*-nitro-phenyl-phosphate (p-NPP), while the Zn_2 form is not. Both derivatives were crystallized and their structures were solved at 2.0 and 2.6 Å resolution for the manganese and zinc derivatives, respectively. The presence of either two Mn^{2+} ions or two Zn^{2+} ions in the metal site was confirmed by X-ray fluorescence and anomalous Fourier difference maps.

The structures of Mn_2PP5c and Zn_2PP5c have an rmsd of 0.21 Å from one another, and the catalytic sites are perfectly superimposable (Figure 2A,B). Each of the two metal ions is coordinated by five ligands. Asp242, His244, and W2 coordinate M1, and Asn303, His352, and His427 coordinate M2, while the carboxylate oxygen of Asp271 and a water molecule (W1) coordinate both M1 and M2. The two metals are 3.3 Å apart. This metal binding site corresponds to the one already reported in the literature for PP5[29] except for the presence in the previous structure of a phosphate ion, which provides an additional oxygen atom as a ligand for both metals.

Complexes with Cantharidin, Cantharidic Acid, Norcantharidin, and Endothall. The structures of Mn_2PP5c soaked with cantharidin, cantharidic acid, norcantharidin, and endothall (Figure 1) have been solved to a resolution of 1.3, 1.6, 1.4, and 1.9 Å, respectively. The structures are of very good quality and the overall rmsd of the protein part with free Mn_2PP5c is 0.14, 0.15, 0.15, and 0.16 Å for the cantharidin, norcantharidin, cantharidic acid, and endothall complexes, respectively.

Cantharidin sits in the catalytic site in its open form (i.e., as a cantharidic acid molecule). Metal M1 is coordinated by three cantharidin oxygens (by one oxygen from each

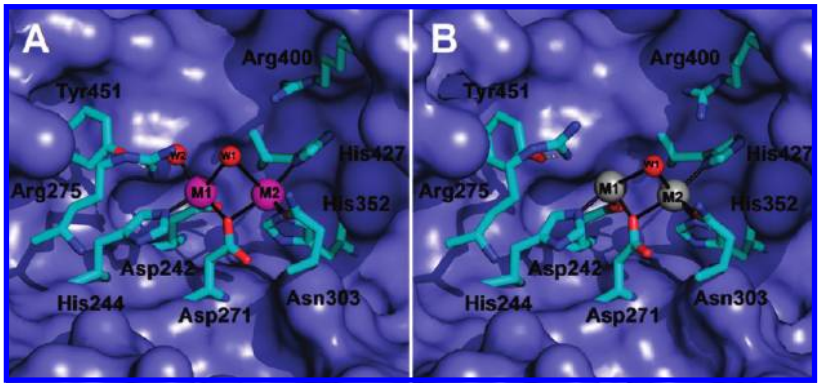

Figure 2. Active site structure of the catalytic domain of PP5. In Mn_2PP5, one metal ion (M1) is coordinated by Asp242, His244, Asp271, and by a water molecule (W2). The other metal ion (M2) is coordinated by Asp271, Asn303, His352, and His427. A further solvent-donated ligand (W1), presumably a hydroxide ion, bridges the two metal ions (A). The active site of Zn_2PP5 exhibits the same structural features of Mn_2PP5 except for the water molecule coordinating the metal ion M1 that is not clearly appreciable in this structure (B).

carboxylate moiety and by the furanic ring oxygen), while metal M2 is coordinated by only one of the carboxylate oxygens, which is bridging with M1. The two carboxylic moieties, which are very close to each other in the adduct, replace all the water molecules, which complete the metal coordination in the dinuclear site in the uninhibited enzyme (cf. Figure 3). Furthermore, in all cases, a double conformation is present in about 50:50 ratio (Figure 3A,B and C,D): while one of the oxygens of each carboxylic acid moiety is still coordinating a metal ion and does not change its position, the other two noncoordinating oxygens bascule in concert with one another in order to maximize the distance between the negatively charged groups. Metal coordination is not affected by this conformational equilibrium, while the side chains of Arg275 and Tyr451 appear to follow the different orientation of the ligand carboxylic groups. By soaking Mn_2PP5c with cantharidic acid practically identical

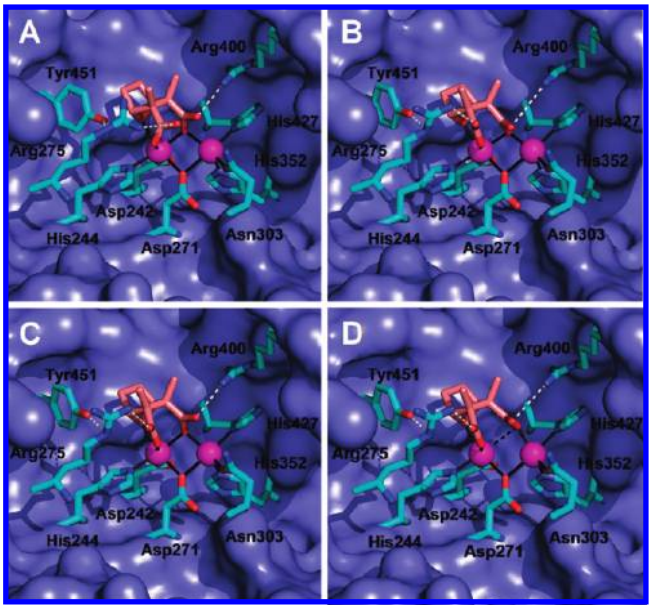

Figure 3. Two different conformations of the active site structure of the catalytic domain of Mn_2PP5 complexed with cantharidin (A,B). Two different conformations of the active site structure of the catalytic domain of Mn_2PP5 complexed with cantharidic acid (C,D). Metal coordination is not affected by this conformational equilibrium, except for the more asymmetric bridging behavior of one of the ligand carboxylic oxygens in (D), while the side chains of Arg275 and Tyr451 appear to follow the different orientation of the ligand carboxylic groups.

structures are obtained, although in this case the two conformations are populated in a 80:20 ratio (Figure 3C,D).

The catalytic site of Mn_2PP5c complexed with norcantharidin is shown in Figure 4A. As observed for cantharidin, norcantharidin sits in the catalytic site in its open form (i.e., as an endothall molecule) and with a similar pose. However, at variance with cantharidin and cantharidic acid, a single conformation is obtained. Apparently, the lack of the two methyl groups allows norcantharidin to select a less strained binding pose with respect to cantharidin.

In all cases, the ligands fit nicely in a small, largely hydrophobic pocket defined by the side chains of Tyr272, Val429, and Phe260 and the backbone atoms of Gln242. The positively charged Arg89 and Arg 214 side chains act as gatekeepers of this hydrophobic cavity and likely stabilize the two metal-coordinated carboxylate groups.

By soaking directly endothall in the catalytic site of Mn_2PP5c, two conformations are obtained, populated in a ratio of about 70:30. In the less populated conformation (Figure 4B), the structure is very similar to those discussed so far for cantharidin, cantharidic acid, and norcantharidin. Surprisingly, in the most populated one (Figure 4C), endothall appears to be rotated by ca. 120° with respect to all the other structures. In this case, the hydrophobic part of the ligand is pointing out of the hydrophobic cavity. This different binding mode of the doubly negatively charged endothall with respect to neutral norcantharidin might suggest that the more hydrophobic part of norcantharidin may initially bind to the hydrophobic cavity and, once bound, be hydrolyzed to endothall. Conversely, endothall as such could be driven into the active site by electrostatic guidance, i.e., the two carboxylate groups being attracted by the two arginine gatekeepers and by the dimetallic site itself. In turn, this would suggest that ligands of this type, which are reported to spontaneously hydrolyze in solution but only on the time scale of tens of minutes,[53] might actually initially bind as anhydrides. Binding as anhydrides could also explain the somewhat different potency observed in vitro for the anhydride and dicarboxylic forms.[53] The alternate binding observed for endothall is not found for the hydrolyzed form of cantharidin, cantharidic acid, possibly either because the two additional methyl groups increase the overall hydrophobicity of the molecule and stabilize its location in the hydrophobic pocket or because the alternate binding pose is sterically less favorable.

The fact that Arg275 adopts two different conformations in the complex with cantharidic acid, and in both cases

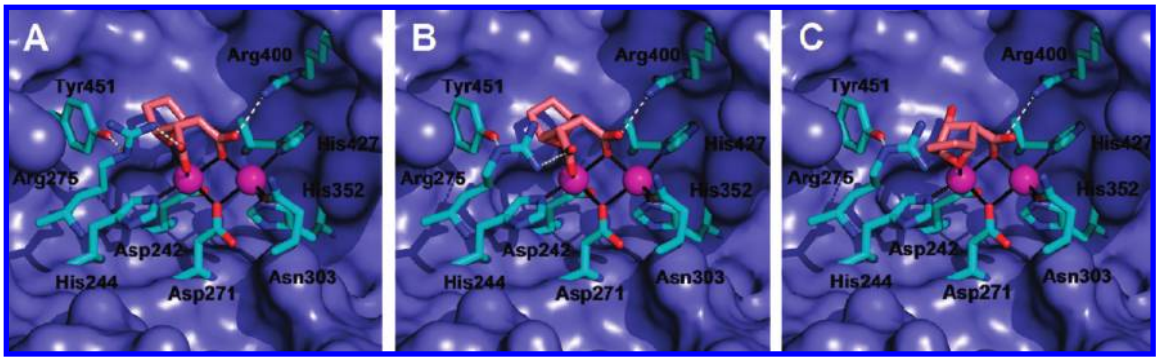

Figure 4. Active site structure of the catalytic domain of Mn_2PP5 complexed with norcantharidin (A). Two different conformations of the active site structure of the catalytic domain of Mn_2PP5 complexed with endothall (B,C). The ligand conformation in C is uniquely different from all other conformations observed in this study.

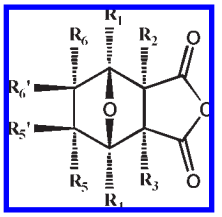

Figure 5. 7-Oxabicyclo[2.2.1]heptane-2,3-dicarboxylic anhydride skeleton with its R_1, R_2, R_3, R_4, R_5, $R_{5'}$, R_6, and $R_{6'}$ substituents.

H-bonded to one of the ligand carboxylic oxygens, suggests that this residue does not only help in stabilizing the inhibitor position in the active site by following its movements, but may also help in stabilizing the bound substrate through at least part of its movements during the catalytic cycle. Conformational freedom of Arg275 seems indeed to be a common feature of the catalytic site of many phosphatases.[30−33] Superimposition of the crystal structures of related phosphatases shows that the amino acids forming the active site are highly conserved. At the same time, the relative mobility of the side chain of Arg275 is maintained.

Complexes of the inhibitors cantharidin, endothall, and cantharidic acid with the inactive Zn_2PP5c have been also obtained (data not shown). The complexes are identical to those with Mn_2PP5c, showing that the nature of the active site metal is irrelevant for even the subtleties of the binding mode of this class of inhibitors.

In summary, it is apparent that the binding modes of cantharidin/norcantharidin in their free acid forms observed here, besides minor differences among them, are in all cases sizably different from previous predictions based on either docking or analogy with higher molecular weight toxins.

The binding pose of the inhibitors in the active site of the enzyme is helpful to explain the experimental affinity constants reported for several cantharidin analogues. Actually, the decoration of the bicyclic scaffold on position R_1, R_4, $R_{5'}$, and $R_{6'}$ (Figure 5) results in a general decrease in binding affinity for all the tested phosphatases[40,53,54] as a consequence of steric clashes with the wall of the active site pocket that are now easily predictable from the present structures. The crystal structures highlight the critical role of the ether oxygen of the oxabicyclic scaffold for the metal binding, and thus explain the decrease in affinity observed in the compounds where the oxygen is replaced by a carbon atom or completely missing.[40] The replacement of one of the metal binding carboxylates with amide derivatives generally worsens the binding affinity.[9] This agrees with the involvement of both the negatively charged carboxylates in metal binding and with the lower binding capability of the amide oxygens for transition metal ions. At the same time, the structures suggest positions R_2 and R_3 as suitable to insert bulkier substituents. Actually, the methyl groups at these positions stick out from the pocket toward the solvent. This is in agreement with the good affinity constant obtained for the 2,3-trimethylene anhydride derivatives where the two methyl groups are linked in a five-membered cycle.[53] The absence of interactions between the amino acids forming the active site and the methyl groups in R_2 and R_3 is consistent with the modest decrease in binding affinity observed in the demethylated derivatives.[55]

Conclusions

In conclusion, the structures of the complexes of cantharidin and of norcantharidin with PP5, a representative member of the Ser/Thr phosphatase family, have been solved for the first time. The analysis of the protein−ligand complexes reveals the structural determinants of the interaction and lays the ground for a structure-based design of new derivatives. In particular, it is shown that the open forms of cantharidin and norcantharidin (cantharidic acid and endothall, respectively) are the real inhibitors of PP5. Hydrolysis may occur upon binding and determines the ligand conformation in the active site. An unexpected feature is the observation of a totally different binding pose for the dicarboxylic form of norcantharidin (endothall) with respect to the very same molecule when formed by in-site hydrolysis of the anhydride. This observation suggests that administration of the anhydride vs the dicarboxylic form of norcantharidin, besides likely differences in pharmacokinetics in vivo, might also result into an intrinsically different binding mode to its molecular target. Moreover, substitutions on position R_2 and R_3 should be preferred to generate new analogues without affecting the optimal binding mode of the cantharidic scaffold.

Finally, the entire set of the present structures reveals a marked plasticity of the catalytic site, which is possibly a common characteristic of all the members of the family. In particular, the capability of Arg275 to move inside the catalytic site to establish new interactions can provide a further anchoring site to the substrate and can be exploited to increase the affinity and the selectivity of new cantharidin-based drugs.

Experimental Section

Plasmid DNA containing the gene of the human full length PP5 enzyme was kindly provided by Prof. D. Barford. The catalytic domain of PP5 (PP5c) corresponding to the 169−449 construct was cloned in the expression vector pDEST30 by Gateway technology and expressed in soluble form in *E. coli* BL21(DE3) RIPL. The growing conditions were optimized in fermentors and the GST-fused protein was purified by means of both affinity and size exclusion chromatography after the removal of the tag. Samples of the purified PP5 protein were dialyzed against a solution containing $MnCl_2$ in order to produce a Mn_2PP5c enzyme. ICP-MS (inductively coupled plasma mass spectrometry) was performed to verify the metal content. The enzymatic activity of the dialyzed sample was assayed by monitoring the dephosphorylation of the *p*-nitro-phenyl-phosphate (pNPP) substrate. The inhibition of dephosphorylation of pNPP was monitored after the addition of selected compounds to the reaction mixture. Crystals of Mn_2PP5c were obtained using the vapor diffusion technique at 16 °C from a 1.1 mM Mn_2PP5c solution containing 10 mM Tris-HCl pH 8.0, 40% MPD ,and 20% PEG MME 5000. Crystals of Mn_2PP5c in complex with the inhibitors cantharidin, norcantharidin, cantharidic acid, and endothall were obtained by soaking Mn_2PP5c crystals with the mother liquor containing the inhibitor itself. The data sets were measured either in-house, using a PX-Ultra copper sealed tube source (Oxford Diffraction) equipped with an Onyx CCD detector, or using synchrotron radiation at BM16, ID14-2, ID23-1 beamlines (ESRF, Grenoble, France). All data sets were collected at 100 K, and the crystals used for data collection were cryocooled without any cryoprotectant treatment. The data were processed in all cases using the program MOSFLM[43] and scaled using the program SCALA[44] with the TAILS and SECONDARY corrections (the latter restrained with a TIE SURFACE command) to achieve an empirical absorption correction. Tables S1, S2, and S3 (see Supporting Information) show the data collection and processing statistics for all data sets. The structures were solved using the molecular replacement technique; the model used for all data sets was 1S95, where water molecules and ions were omitted. The correct orientation and translation of the molecule within the crystallographic unit cell was determined with standard

Patterson search techniques[45,46] as implemented in the program MOLREP.[47,48] The isotropic refinement was carried out using REFMAC5[49] on all data sets. REFMAC5 default weights for the crystallographic and the geometrical term have been used in all cases. In between the refinement cycles, the models were subjected to manual rebuilding by using XtalView.[50] The same program was used to manually build the inhibitor molecules. Water molecules were added by using the standard procedures within the ARP/WARP suite.[51] The stereochemical quality of the refined models was assessed using the program Procheck.[52] The Ramachandran plots are in all cases of good quality.

Acknowledgment. This work was supported by EC (projects: MEST-CT-2004-504391, SFMET no. 201640, SPINE2-COMPLEXES no. 031220, and Nano4Drugs no. LSHB-CT-2005-019102), by MIUR (PRIN 2005, Prot. N. 2005039878, Prot. RBLA032ZM7, Prot. RBIP06LSS2), and Ente Cassa di Risparmio di Firenze.

Supporting Information Available: Data collection and refinement statistics for PP5c structures. This material is available free of charge via the Internet at http://pubs.acs.org.

References

(1) Li, Y. M.; Casida, J. E. Cantharidin-Binding Protein—Identification As Protein Phosphatase-2A. *Proc. Natl. Acad. Sci. U.S.A.* **1992**, *89*, 11867–11870.
(2) Chen, Y. N.; Chen, J. C.; Yin, S. C.; Wang, G. S.; Tsauer, W.; Hsu, S. F.; Hsu, S. L. Effector mechanisms of norcantharidin-induced mitotic arrest and apoptosis in human hepatoma cells. *Int. J. Cancer* **2002**, *100*, 158–165.
(3) Efferth, T.; Rauh, R.; Kahl, S.; Tomicic, M.; Bochzelt, H.; Tome, M. E.; Briehl, M. M.; Bauer, R.; Kaina, B. Molecular modes of action of cantharidin in tumor cells. *Biochem. Pharmacol*. **2005**, *69*, 811–818.
(4) Rauh, R.; Kahl, S.; Boechzelt, H.; Bauer, R.; Kaina, B.; Efferth, T. Molecular biology of cantharidin in cancer cells. *Chin. Med*. **2007**, *2*, 8.
(5) Dorn, D. C.; Kou, C. A.; Png, K. J.; and Moore, M. A. The effect of cantharidins on leukemic stem cells. *Int. J. Cancer* **2008**.
(6) Chen, Y. N.; Cheng, C. C.; Chen, J. C.; Tsauer, W.; Hsu, S. L. Norcantharidin-induced apoptosis is via the extracellular signal-regulated kinase and c-Jun-NH2-terminal kinase signaling pathways in human hepatoma HepG2 cells. *Br. J. Pharmacol*. **2003**, *140*, 461–470.
(7) Sagawa, M.; Nakazato, T.; Uchida, H.; Ikeda, Y.; Kizaki, M. Cantharidin induces apoptosis of human multiple myeloma cells via inhibition of the JAK/STAT pathway. *Cancer Sci*. **2008**, *99*, 1820–1826.
(8) Kok, S. H.; Cheng, S. J.; Hong, C. Y.; Lee, J. J.; Lin, S. K.; Kuo, Y. S.; Chiang, C. P.; Kuo, M. Y. Norcantharidin-induced apoptosis in oral cancer cells is associated with an increase of proapoptotic to antiapoptotic protein ratio. *Cancer Lett*. **2005**, *217*, 43–52.
(9) Hill, T. A.; Stewart, S. G.; Gordon, C. P.; Ackland, S. P.; Gilbert, J.; Sauer, B.; Sakoff, J. A.; McCluskey, A. Norcantharidin analogues: synthesis, anticancer activity and protein phosphatase 1 and 2A inhibition. *ChemMedChem* **2008**, *3*, 1878–1892.
(10) Norbury, C. J.; Zhivotovsky, B. DNA damage-induced apoptosis. *Oncogene* **2004**, *23*, 2797–2808.
(11) Slee, E. A.; O'Connor, D. J.; Lu, X. To die or not to die: how does p53 decide?. *Oncogene* **2004**, *23*, 2809–2818.
(12) Babine, R. E.; Bender, S. L. Molecular Recognition of Protein−Ligand Complexes: Applications to Drug Design. *Chem. Rev*. **1997**, *97*, 1359–1472.
(13) Aureli, L.; Gioia, M.; Cerbara, I.; Monaco, S.; Fasciglione, G. F.; Marini, S.; Ascenzi, P.; Topai, A.; Coletta, M. Structural bases for substrate and inhibitor recognition by matrix metalloproteinases. *Curr. Med. Chem*. **2008**, *15*, 2192–2222.
(14) Knapp, J.; Boknik, P.; Huke, S.; Gombosova, I.; Linck, B.; Luss, H.; Muller, F. U.; Muller, T.; Nacke, P.; Schmitz, W.; Vahlensieck, U.; Neumann, J. Contractility and inhibition of protein phosphatases by cantharidin. *Gen. Pharmacol*. **1998**, *31*, 729–733.
(15) McCluskey, A.; Sakoff, J. A. Small molecule inhibitors of serine/threonine protein phosphatases. *Mini. Rev. Med. Chem*. **2001**, *1*, 43–55.
(16) Melnikova, I.; Golden, J. Targeting protein kinases. *Nat. Rev. Drug Discovery* **2004**, *3*, 993–994.
(17) Ventura, J. J.; Nebreda, A. R. Protein kinases and phosphatases as therapeutic targets in cancer. *Clin. Transl. Oncol*. **2006**, *8*, 153–160.
(18) Sawyer, T. K.; Shakespeare, W. C.; Wang, Y.; Sundaramoorthi, R.; Huang, W. S.; Metcalf, C. A.III; Thomas, M.; Lawrence, B. M.; Rozamus, L.; Noehre, J.; Zhu, X.; Narula, S.; Bohacek, R. S.; Weigele, M.; Dalgarno, D. C. Protein phosphorylation and signal transduction modulation: chemistry perspectives for small-molecule drug discovery. *Med. Chem*. **2005**, *1*, 293–319.
(19) Vazquez, J.; Tautz, L.; Ryan, J. J.; Vuori, K.; Mustelin, T.; Pellecchia, M. Development of Molecular Probes for Second-Site Screening and Design of Protein Tyrosine Phosphatase Inhibitors. *J. Med. Chem*. **2007**, *50*, 2137–2143.
(20) Barford, D.; Das, A. K.; Egloff, M. P. The structure and mechanism of protein phosphatases: insights into catalysis and regulation. *Annu. Rev. Biophys. Biomol. Struct*. **1998**, *27*, 133–164.
(21) Hinds, T. D. Jr.; Sanchez, E. R. Protein phosphatase 5. *Int. J. Biochem. Cell Biol*. **2008**, *40*, 2358–2362.
(22) Kennelly, P. J. Protein phosphatases—a phylogenetic perspective. *Chem. Rev*. **2001**, *101*, 2291–2312.
(23) McConnell, J. L.; Wadzinski, B. E. Targeting protein serine/threonine phosphatases for drug development. *Mol. Pharmacol*. **2009**, *75*, 1249–1261.
(24) Barton, G. J.; Cohen, P. T. W.; Barford, D. Conservation Analysis and Structure Prediction of the Protein Serine/Threonine Phosphatases—Sequence Similarity with Diadenosine Tetraphosphatase from *Escherichia coli* Suggests Homology to the Protein Phosphatases. *Eur. J. Biochem*. **1994**, *220*, 225–237.
(25) Barford, D. Molecular mechanisms of the protein serine threonine phosphatases. *Trends Biochem. Sci*. **1996**, *21*, 407–412.
(26) Chen, M. X.; McPartlin, A. E.; Brown, L.; Chen, Y. H.; Barker, H. M.; Cohen, P. T. W. A Novel Human Protein Serine/Threonine Phosphatase, Which Possesses 4 Tetratricopeptide Repeat Motifs and Localizes to the Nucleus. *EMBO J*. **1994**, *13*, 4278–4290.
(27) McCluskey, A.; Sim, A. T.; Sakoff, J. A. Serine−threonine protein phosphatase inhibitors: development of potential therapeutic strategies. *J. Med. Chem*. **2002**, *45*, 1151–1175.
(28) Yang, J.; Roe, S. M.; Cliff, M. J.; Williams, M. A.; Ladbury, J. E.; Cohen, P. T. W.; Barford, D. Molecular basis for TPR domain-mediated regulation of protein phosphatase. *EMBO J*. **2005**, *24*, 1–10.
(29) Swingle, M. R.; Honkanen, R. E.; Ciszak, E. M. Structural basis for the catalytic activity of human serine/threonine protein phosphatase-5. *J. Biol. Chem*. **2004**, *279*, 33992–33999.
(30) Kelker, M. S.; Page, R.; Peti, W. Crystal structures of protein phosphatase-1 bound to nodularin-R and tautomycin: a novel scaffold for structure-based drug design of serine/threonine phosphatase inhibitors. *J. Mol. Biol*. **2009**, *385*, 11–21.
(31) Maynes, J. T.; Luu, H. A.; Cherney, M. M.; Andersen, R. J.; Williams, D.; Holmes, C. F.; James, M. N. Crystal structures of protein phosphatase-1 bound to motuporin and dihydromicrocystin-LA: elucidation of the mechanism of enzyme inhibition by cyanobacterial toxins. *J. Mol. Biol*. **2006**, *356*, 111–120.
(32) Xing, Y.; Xu, Y.; Chen, Y.; Jeffrey, P. D.; Chao, Y.; Lin, Z.; Li, Z.; Strack, S.; Stock, J. B.; Shi, Y. Structure of protein phosphatase 2A core enzyme bound to tumor-inducing toxins. *Cell* **2006**, *127*, 341–353.
(33) Li, H.; Zhang, L.; Rao, A.; Harrison, S. C.; Hogan, P. G. Structure of calcineurin in complex with PVIVIT peptide: portrait of a low-affinity signalling interaction. *J. Mol. Biol*. **2007**, *369*, 1296–1306.
(34) Swingle, M.; Ni, L.; Honkanen, R. E. Small-molecule inhibitors of Ser/Thr protein phosphatases: specificity, use and common forms of abuse. *Methods Mol. Biol*. **2007**, *365*, 23–38.
(35) Maynes, J. T.; Bateman, K. S.; Cherney, M. M.; Das, A. K.; Luu, H. A.; Holmes, C. F.; James, M. N. Crystal structure of the tumor-promoter okadaic acid bound to protein phosphatase-1. *J. Biol. Chem*. **2001**, *276*, 44078–44082.
(36) Maynes, J. T.; Perreault, K. R.; Cherney, M. M.; Luu, H. A.; James, M. N.; Holmes, C. F. Crystal structure and mutagenesis of a protein phosphatase-1:calcineurin hybrid elucidate the role of the beta12-beta13 loop in inhibitor binding. *J. Biol. Chem*. **2004**, *279*, 43198–43206.
(37) Xing, Y.; Xu, Y.; Chen, Y.; Jeffrey, P. D.; Chao, Y.; Lin, Z.; Li, Z.; Strack, S.; Stock, J. B.; Shi, Y. Structure of protein phosphatase 2A core enzyme bound to tumor-inducing toxins. *Cell* **2006**, *127*, 341–353.
(38) Kita, A.; Matsunaga, S.; Takai, A.; Kataiwa, H.; Wakimoto, T.; Fusetani, N.; Isobe, M.; Miki, K. Crystal structure of the complex between calyculin A and the catalytic subunit of protein phosphatase 1. *Structure* **2002**, *10*, 715–724.

(39) Baba, Y.; Hirukawa, N.; Tanohira, N.; Sodeoka, M. Structure-based design of a highly selective catalytic site-directed inhibitor of Ser/Thr protein phosphatase 2B (calcineurin). *J. Am. Chem. Soc.* **2003**, *125*, 9740–9749.
(40) McCluskey, A.; Keane, M. A.; Mudgee, L. M.; Sim, A. T. R.; Sakoff, J.; Quinn, R. J. Anhydride modified cantharidin analogues. Is ring opening important in the inhibition of protein phosphatase 2A?. *Eur. J. Med. Chem.* **2000**, *35*, 957–964.
(41) Gauss, C. M.; Sheppeck, J. E.; Nairn, A. C.; Chamberlin, R. A molecular modeling analysis of the binding interactions between the okadaic acid class of natural product inhibitors and the Ser-Thr phosphatases, PP1 and PP2A. *Bioorg. Med. Chem.* **1997**, *5*, 1751–1773.
(42) Bertini, I.; Fragai, M.; Luchinat, C.; Talluri, E. Water-based ligand screening for paramagnetic metalloproteins. *Angew. Chem., Int. Ed.* **2008**, *47*, 4533–4537.
(43) Leslie,A. G. W. Crystallographic Computing V. In Molecular Data Processing; Moras, D., Podjarny, A. D., Thierry, J.-C., Eds.; Oxford University Press: Oxford, 1991; pp 50−61.
(44) Evans, P. R. Data Reduction, Proceedings of CCP4 Study Weekend. *Data Collect. Process.* **1993**, 114−122. Conference Proceeding.
(45) Rossmann, M. G.; Blow, D. M. The detection of sub-units within the crystallographic asymmetric unit. *Acta Crystallogr., Sect. D: Biol. Crystallogr.* **1962**, *15*, 24–31.
(46) Crowther,R. A. The Molecular Replacement Method. Rossmann, M. G. Ed.; Gordon & Breach: New York, 1972.
(47) Vagin, A.; Teplyakov, A. MOLREP: an automated program for molecular replacement. *J. Appl. Crystallogr.* **1997**, *30*, 1022–1025.
(48) Vagin, A.; Teplyakov, A. An approach to multi-copy search in molecular replacement. *Acta Crystallogr., Sect. D: Biol. Crystallogr.* **2000**, *56*, 1622–1624.
(49) Murshudov, G. N.; Vagin, A. A.; Dodson, E. J. Refinement of macromolecular structures by the maximum-likelihood method. *Acta Crystallogr., Sect. D: Biol. Crystallogr.* **1997**, *53*, 240–255.
(50) McRee, D. E. XtalView: A Visual Protein Crystallographic Software System for XII/XView. *J. Mol. Graphics* **1992**, *10*, 44–47.
(51) Lamzin, V. S.; Wilson, K. S. Automated refinement of protein models. *Acta Crystallogr., Sect. D: Biol. Crystallogr.* **1993**, *49*, 129–147.
(52) Laskowski, R. A.; MacArthur, M. W.; Moss, D. S.; Thornton, J. M. PROCHECK: a program to check the stereochemical quality of protein structures. *J. Appl. Crystallogr.* **1993**, *26*, 283–291.
(53) McCluskey, A.; Taylor, C.; Quinn, R. J.; Suganuma, M.; Fujiki, H. Inhibition of Protein Phosphatase 2A by Cantharidin. *Bioorg. Med. Chem. Lett.* **1996**, *6*, 1025–1028.
(54) Baba, Y.; Hirukawa, N.; Sodeoka, M. Optically active cantharidin analogues possessing selective inhibitory activity on Ser/Thr protein phosphatase 2B (calcineurin): Implications for the binding mode. *Bioorg. Med. Chem. Lett.* **2005**, *13*, 5164–5170.
(55) Sheppeck, J. E.; Gauss, C. M.; Chamberlin, A. R. Inhibition of the Ser-Thr phosphatases PP1 and PP2A by naturally occurring toxins. *Bioorg. Med. Chem.* **1997**, *5*, 1739–1750.